On the relationship between SiF_4 plasma species and sample properties in ultra low-k etching processes

Cite as: AIP Advances 10, 065212 (2020); doi: 10.1063/1.5125498
Submitted: 23 August 2019 • Accepted: 13 May 2020 •
Published Online: 8 June 2020

Micha Haase,[1,a)] Marcel Melzer,[2] Norbert Lang,[3] Ramona Ecke,[1] Sven Zimmermann,[1,2] Jean-Pierre H. van Helden,[3] and Stefan E. Schulz[1,2]

AFFILIATIONS

[1]Fraunhofer Institute for Electronic Nano Systems, Technologie-Campus 3, D-09126 Chemnitz, Germany
[2]Chemnitz University of Technology, Center for Microtechnologies, D-09107 Chemnitz, Germany
[3]Leibniz Institute for Plasma Science and Technology, Felix-Hausdorff-Str. 2, D-17489 Greifswald, Germany

[a)]**Author to whom correspondence should be addressed:** micha.haase@enas.fraunhofer.de

ABSTRACT

The temporal behavior of the molecular etching product SiF_4 in fluorocarbon-based plasmas used for the dry etching of ultra low-k (ULK) materials has been brought into connection with the polymer deposition on the surface during plasma treatment within the scope of this work. For this purpose, time-resolved measurements of the density of SiF_4 have been performed by quantum cascade laser absorption spectroscopy. A quantification of the non-linear time dependence was achieved by its characterization via a time constant of the decreasing SiF_4 density over the process time. The time constant predicts how fast the stationary SiF_4 density is reached. The higher the time constant is, the thicker the polymer film on top of the treated ultra low-k surface. A correlation between the time constant and the ULK damage was also found. ULK damage and polymer deposition were proven by Variable Angle Spectroscopic Ellipsometry and X-ray Photoelectron Spectroscopy. In summary, the observed decay of the etching product concentration over process time is caused by the suppressed desorption of the SiF_4 molecules due to a more dominant adsorption of polymers.

I. INTRODUCTON

The requirements of plasma etching processes in semiconductor chip manufacturing become more and more challenging. Stable plasma process conditions, run to run uniformity, fault detection, and conditioning or seasoning problems are well-known challenges with which companies have to deal every day. To overcome these problems, plasma diagnostic methods were introduced to control the process plasmas. Probably, the most common method is optical emission spectroscopy (OES), which is mainly used for end point detection in dry etching processes. In 1998, Klick *et al.*[1] introduced the usage of the self-excited electron resonance spectroscopy (SEERS) as a kind of plasma diagnostics. In this study, the authors demonstrated the determination of the parameter plasma electron density and electron collision frequency. They showed an excellent agreement of the electron densities determined with Langmuir probe and SEERS in different gas discharges,[1] thus, opening the possibility to measure this electrical plasma parameter non-invasively in process plasmas. Today, the SEERS sensor is widely applied on etch reactors and can be used as the fault detection system as it was already proposed by Baek *et al.* in 2005.[2] In their study, inductive coupled plasma (ICP) etching processes of tungsten-silicide were investigated, and they elaborated the link between the etched profile and the electron collision rate. This is a very good example of combined analysis of *in situ* and *ex situ* process results. It is also described in literature that the effective collision frequency evolved to a criterion of reproducibility.[3] Baek and co-workers explored the chamber state with respect to the conditioning of the process reactor and focused their investigation on the so-called first wafer effect, which was qualified by comparing certain plasma parameters of sequential (simplified) plasma processes.[4] In this study, the first wafer effect could not be proven

with OES. The authors attributed this fact to the limitation of this *in situ* diagnostics, which only measured the information on the plasma bulk. Instead of measuring electrical plasma parameters, Lang *et al.* applied an absorption measurement method on fluorocarbon-based plasmas for dry etching of porous dielectric materials.[5] They were also able to detect the conditioning state of the process chamber by comparing the concentration of the etching by-product carbon monoxide of cleaned and non-cleaned process chambers. The mentioned literature demonstrates the importance of diagnostics in plasma processes for semiconductor applications.

However, not only the plasma parameters themselves are important. The most essential output parameter is the process result, i.e., the sample properties after plasma treatment. The task should also be to compare the *in situ* plasma information with the sample properties.[6] As an example, Hübner *et al.*[7] investigated the CF_2 radical density in dielectric etching processes with the result, in which changes in the CF_2 concentration correlates with the sample structure itself. It should be pointed out here that Hübner as well as Lang investigated dry etching processes of porous SiOCH, an ultra low-k (ULK) material, with a k-value lower than 3.9. The patterning of such porous material is highly challenging because of the well-known plasma induced ULK damage. This term refers to the degradation of the material caused by the plasma process. Very good overviews on the damage mechanisms are given in the publications of Baklanov *et al.*[8,9] According to several other authors, damage could be explained by the loss of methyl groups from the material[10] or surface fluorination and hydrogen abstraction by fluorine atoms.[11] Further damage is observed due to carbon depletion and resulting formation of dangling bonds with subsequent formation of silanol groups due to the exposure to the atmosphere.[12,13] Summarizing, each damage mechanism leads to the same result—an increase in the dielectric constant of the material. Caused by the complexity of the plasma induced ULK damage (radicals, ions, and radiation lead separately and in combination with each other to a degradation of the ULK[14]), the ULK etching process is a very good representative for combined analysis of *in situ* and *ex situ* process information.

In order to analyze the *in situ* measured molecular concentrations and their influence on the properties of the treated samples, ULK etching processes were investigated by quantum cascade laser absorption spectroscopy (QCLAS). In particular, the density of the plasma etching product SiF_4 was measured during the reactive ion etching (RIE) process and analyzed with regard to its development over time. The partially etched ULK samples were characterized with Variable Angle Spectroscopic Ellipsometry (VASE) to determine the optical constants and thicknesses of the modified film stack. X-ray Photoelectron Spectroscopy (XPS) measurements were performed to analyze the atomic surface compositions and surface species of the plasma treated ULK. To characterize the temporal behavior of the SiF_4 density, an exponential time constant could be introduced to quantify its decay and to explain the interrelation between the sample properties and the stable etching product SiF_4.

II. EXPERIMENTAL DETAILS

The experimental investigations are a combination of several parts. First, the plasma treatment of the samples with simultaneous measurement of the etching product SiF_4 has been performed. The second part of the study was the characterization of the sample properties after the plasma etching process by the determination of refractive indices and thicknesses using VASE, while the third part was the measurement of the surface composition and species of the partially etched surfaces via XPS. In Subsections II A–II D, the processes and analytical methods are described in detail.

A. Sample treatment

For the study, a 500 nm thick porous SiOCH layer, with a dielectric constant of 2.4, was chosen and deposited on silicon by plasma-enhanced chemical vapor deposition. The provided samples were 300 mm wafers, which had to be cut into square pieces of a size of 10 cm × 10 cm to process them in a system for 8 in. wafers. The samples were etched in a magnetic enhanced reactive ion etch (MERIE) chamber of a Centura 5200 cluster system (Applied Materials). Because of the sample size, each sample had been placed on 200 mm adapter wafers to be transferred through the used 200 mm cluster tool. In order not to influence the SiF_4 density during the absorption measurements, all adapter wafers were coated with aluminum.

A kind of simplex diagram was designed as parameter space for this study. To investigate the effect of the gases, CF_4, CHF_3, and Ar were varied within the range from 0 sccm to 100 sccm, keeping the total flow constant. The stoichiometric fluorine to carbon ratio of the precursor gas was defined by the gas flows of the chemical (Φ_{CF4}) and polymerizing (Φ_{CHF3}) component and is given by

$$F/C = \frac{4\Phi_{CF4} + 3\Phi_{CHF3}}{\Phi_{CF4} + \Phi_{CHF3}}. \quad (1)$$

For all processes, the RIE power and process pressure were kept constant at 600 W and 100 mTorr, respectively. Therefore, the absorption of SiF_4 was measured in processes for which the partial pressure of CF_4 was changed by replacing it with CHF_3 (reduction of F/C) and Ar (dilution of chemistry). To ensure consistent starting conditions, the chamber was cleaned after each ULK etching process with O_2/SF_6 plasma for 100 s.

B. Etching product concentration measurements via QCLAS

For the *in situ* determination of molecular etching product concentrations, a QCLAS spectrometer system from neoplas control GmbH (Q-MACS Process fiber) was coupled to the MERIE plasma reactor. To enhance the sensitivity of the system, a so-called multipass optics (MPO, neoplas control GmbH) consisting of two concave mirrors needed to adjust the number of transitions of the laser beam through the plasma was implemented at the chamber, as illustrated in Fig. 1. Setting up the MPO for 12 transitions, the effective absorption length through the plasma results in 5.4 m. This leads to a limit of detection in the range of 10^{12} molecules cm^{-3}, which corresponds to 300 ppm for the studied pressure range. In plasmas containing fluorine for etching ULK layers, one of the most prominent etching product built is the stable molecule SiF_4.[6,15] To measure the absorption of this plasma species a quantum cascade laser was used, which emits in a range between 1030.90 cm^{-1} and 1031.00 cm^{-1}. For a more detailed description of the QCLAS spectrometer system and the method to determine the concentration of SiF_4 from measured

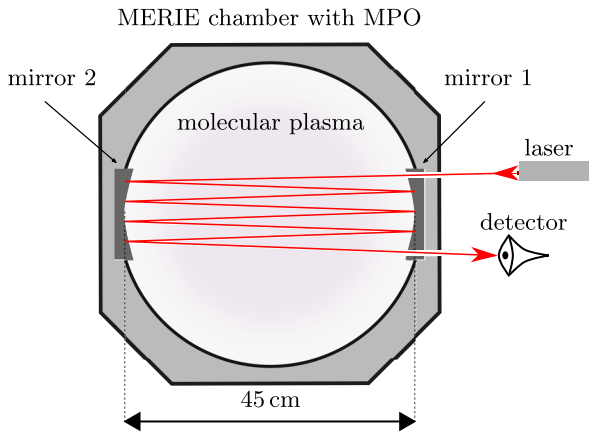

FIG. 1. Schematic of the top view of a modified MERIE chamber with the MPO implemented with a mirror spacing of 45 cm to guide a laser beam up to 12 times through the molecular plasma.

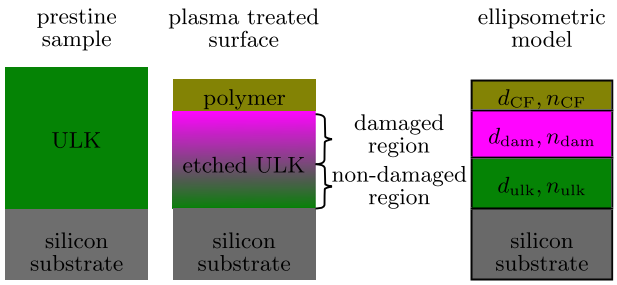

FIG. 2. Schematic comparison of pristine sample (left), partially etched surface (middle), and ellipsometric model (right). The pristine ULK film deposited on a silicon substrate is a single layer. A partially etched ULK consists of a polymer film, damaged and non-damaged regions without a sharp interface between the regions. For the description, a 3 layer model with thicknesses and refractive indices for the polymer film (d_{CF}, n_{CF}), damaged (d_{dam}, n_{dam}) and non-damaged ULK (d_{ULK}, n_{ULK}) is used, respectively.

absorptions, the reader is referred to the paper from Lang *et al.*,[5] where such a QCLAS system was used for the investigation of ULK etching processes in an inductively coupled plasma.

C. Sample characterization via ellipsometry

The characterization of the samples was done at first by using VASE. For this, a SE850 of Sentech GmbH was used. Each VASE measurement was executed with three incident angles (50°, 60°, and 70°) to model a dielectric function of the films. The wavelength range for the measurements was fixed at 400 nm up to 850 nm. For the development of an ellipsometric model of partially etched ULK films, it is necessary to consider two mechanisms, which happens due to the etching process. First, as discussed above, ULK damage occurs during the plasma treatment. Therefore, the ULK consists of damaged and non-damaged regions. Second, due to polymerization during the ULK etching, a polymer layer could be deposited on top of the ULK.[16,17] Hence, the composition of the layer from top to bottom, after applying a fluorocarbon plasma, is a CF polymer followed by a damaged ULK region and non-damaged material underneath, as shown in the middle of Fig. 2. For an accurate ellipsometric model of the partially etched ULK, these properties have to be considered. Thus, a three layer model was used to describe the film after the plasma treatment (Fig. 2, right). A polymer layer can be described with a Lorentz oscillator,[18] which was also done in this study. As already mentioned, the measurements were applied in the VIS region. In this wavelength range, non-damaged ULK material can be modeled with a simple Cauchy layer because the extinction coefficient is zero in this region.[19–21] Damaged ULK is similar to SiO_2 and could be modeled with a Cauchy model, too. However, it was not possible to separate the damaged ULK from the non-damaged ULK using two Cauchy layers on top of each other. Therefore, we decided to describe the damaged ULK property with a single Lorenz oscillator, which can be used to describe the dielectric function of insulating materials, too. The damping parameter, which determines the complex part of the refractive index or the extinction coefficient was of course set to zero.[18] A similar approach to use two separate layers for damaged and non-damaged ULK regions on top of each other is also reported by Nishida.[22] In this study, the Bruggeman's effective medium approximation was used. In order to prevent the usage of too many fit parameters and the fact of not knowing the porosity of the damaged ULK, this model was not used in our study. Additionally, it is advisable to prove the used ellipsometric model, especially when the model has many parameters to describe the measurement date. A common way to estimate the model quality is to check the pairwise non-linearity between all fit parameters. This can be done by the calculation of the correlation matrix, which was done in this study for each single fit result. Only if no correlation between the fit parameters was found, the model was classified as trustable. It should be noted that the ellipsometric model cannot be used to determine the thickness of the damaged and the non-damaged ULK regions. This is due to two reasons: first, a sharp interface between damaged and non-damaged regions does not exist (compare Fig. 2, middle). Second, the isotropic material properties from top to bottom should not be assumed. Therefore, after the VASE measurements of the etched surfaces, the samples were treated in strong diluted hydrogen fluorine solution (HF:H_2O, 1:800) to remove the polymer film on top and the damaged ULK. The treatment time was 600 s. Such an approach will not affect the non-damaged material as shown recently.[24] In this study, blanket ULK films with different damage depths were etched in a diluted hydrogen fluorine solution for different durations. It was found that, for each duration of wet etching, the amount of the removed material remains the same. Therefore, the wet etching process will stop itself if the damaged ULK is removed. The etching of the damaged area will remove the polymer layer on the top at once. Since a non-closed polymer film is expected, the solution can directly access the damaged ULK as it has been reported by Leitsmann *et al.*[25] Their theoretical study shows that the removal of CF polymers from ULK surfaces through the use of diluted HF based solutions is possible if the polymer layers have high porosity. Such an undercutting effect causes the CF film to lift off. After the removal of the damaged areas, the film stack consists of only non-damaged ULK, which was measured again by ellipsometry. Thus, the damage depth was simply calculated by the subtraction of the polymer thickness and the non-damaged ULK thickness from the total film thickness.

TABLE I. Bondings and energies for the elements.[23]

Component	C—C	C—CF_x	C—O	C—F	C—F_2	C—F_3
Energy range (eV)	284.3–284.7	286.1–286.5	287.1–287.5	288.7–289.1	290.7–291.1	292.9–293.3

D. Sample characterization via XPS

To prove the existence of polymer films on top of partially etched ULK samples, the layer composition was analyzed after the dry etching process by X-ray Photoelectron Spectroscopy (XPS). However, a short air contact could not be avoided during the transfer of the samples from the etching tool to the neighbored analysis tool. A R3000 electron energy analyzer with a pass energy of 200 eV and monochromatic Al-Kα radiation from a MX 650 X-ray source both from VG Scienta were used for this purpose. An electron flood gun was applied during the XPS measurement in order to compensate the charging of the isolating low-k samples. The parameters of the flood gun were chosen in such a way that the Si 2p peak was shifted to 103.5 eV binding energy corresponding to SiO_2.[26] For the analysis of the XPS spectra, CasaXPS Version 2.3.16 Pre-rel 1.4 was applied using Scofield relative sensitivity factors in combination with a Shirley background. According to the literature, a value of −0.75 was set for the depth correction.[27–29] For a more detailed examination of the binding conditions of the polymer layers, the carbon peak was decomposed into several peaks (e.g., C—C, C—F, C—F_2). A numerical approximation for a Voigt profile (Lorentz 30% share) was used as a line shape model to determine the respective peaks of the deconvolution. The full width at half maximum (FWHM) has been limited to 1.5–3.0 eV for the deconvolution, and the allowed energy ranges for the peaks can be found in Table I. The respective energy values are based on the overview of Vandencasteele and Reniers.[23]

III. RESULTS AND DISCUSSION

A. SiF_4 densities and their correlation to the etching rate

An example of a time-resolved density measurement of SiF_4 during ULK etch is shown in Fig. 3. This measurement was done with a gas mixture of 25 sccm and 75 sccm for CF_4 and CHF_3, respectively. According to Eq. (1), the corresponding F/C ratio equals to 3.25. The plasma treatment process was started at time t_0. Being a pure etching product SiF_4 could be detected only during the plasma processing of the sample. Depending on the F/C ratio, it was observed that the SiF_4 densities decay during the plasma process despite the process parameters being kept constant. Furthermore, both the mean produced SiF_4 densities and the etching rate scale proportional to the F/C ratio, as shown in Fig. 4. Plotted is the normalized etching rate as well as the normalized SiF_4 density averaged over the entire etching process as a function of the F/C ratio of the precursor gas for different argon flow rates. First of all, both properties show the same dependency on the F/C ratio for each applied Ar flow rate, which proves a strong correlation between the etching rate and SiF_4 density. Furthermore, an increase in the F/C ratio leads to higher etching rates as well as to higher SiF_4 densities. Hence, the reduction of the CF_4 partial pressure by the substitution of CHF_3 lowers the etching rate and the SiF_4 density as well. It is well known that the partial replacement of CF_4 by a polymerizing gas such as CHF_3 reduces the etching rate of porous SiOCH as reported by Posseme *et al.*[17] Lang *et al.* reported a direct proportionality between the etching rate and SiF_4 density.[5] It should be noted that these results are based on the analysis of stationary concentrations the authors observed under different conditions. In contrast, the temporal evolution of the SiF_4 density observed in the present work is highly non-linear. A method to characterize this time-dependent SiF_4 concentration is proposed and discussed later. Plotting the etching rate as a function of the SiF_4 built on average during the plasma process, also a linear dependency was found as shown in Fig. 5. It was observed that the F/C ratio has a significant influence on the temporal behavior of the SiF_4 density during the plasma process. In Fig. 6, the time resolved SiF_4 densities are shown for five different F/C ratios in the entire possible range according to Eq. (1) and a total flow of 100 sccm. As mentioned earlier, due to the reduction of the F/C ratio at a constant total gas flow, the total amount of SiF_4 produced during the plasma process decreases. This could be understood because of a subsequent substitution of the more polymerizing component CHF_3, which leads to a lower etching rate and, thus, to a lower SiF_4 density. Furthermore, the concentration of SiF_4 typically did not remain constant during the plasma process. In order to characterize the observed temporal evolution of the SiF_4, an exponential model was fitted to the data. Although an empirical model, using the following approach, the temporal decay of the SiF_4 could be fitted at best:

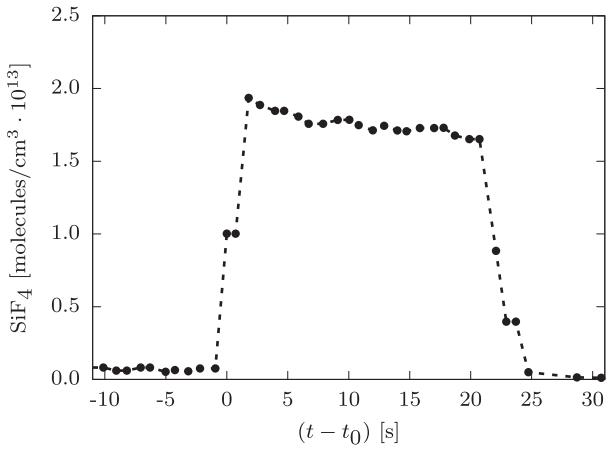

FIG. 3. Time resolved SiF_4 density during an ULK etch process measured with QCLAS under process conditions of 100 mTorr total pressure, 600 W RF power, and a F/C ratio of the precursor gas of 3.25. The plasma process starts at $t = t_0$.

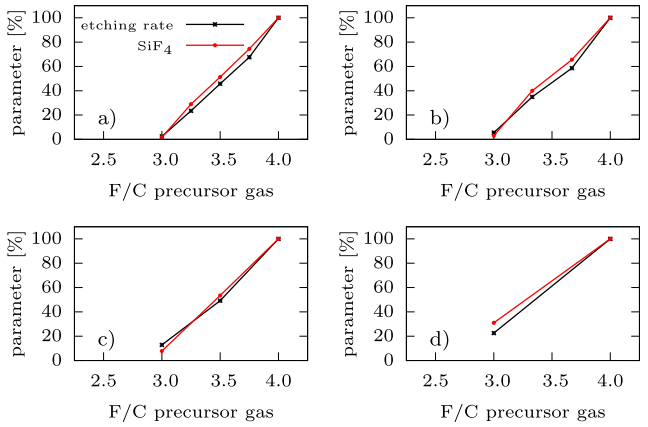

FIG. 4. Comparison of the normalized etching rate and mean SiF_4 densities as a function of the F/C ratio for different Ar flows: (a) 0 sccm, (b) 25 sccm, (c) 50 sccm and (d) 75 sccm. The linearity proves a strong correlation between the etch product density and the etching rate.

$$C_{SiF4}(t) = a + b \cdot e^{c/(t-t_0)}, t > t_0, \quad (2)$$

where $C_{SiF4}(t)$ is the time-dependent SiF_4 concentration, a and b are concentration values, which represent in sum the stationary SiF_4 concentration at the end of the decay, i.e., $C_{SiF4}(stat.) = a + b$, and c is the characteristic time constant. It should be noted that there is still no physical interpretation behind the model. This will be the subject of further investigations. The results of the fit are shown additionally in Fig. 6, including the corresponding values of the time constant c. As a consequence, an increase in the polymerizing component of the precursor gas results in higher decay constants. The uncertainty in the determination of the SiF_4 density of about 10% results in an insensitivity of the fit model to resolve small changes in c leading to its marginal negative change when the F/C ratio changes from 4 to 3.75, see Fig. 6 and upper left graph in Fig. 7, respectively. The characterization depending on the applied Ar flow is summarized in Fig. 7 via plotting the time constant c as a function of the F/C ratio.

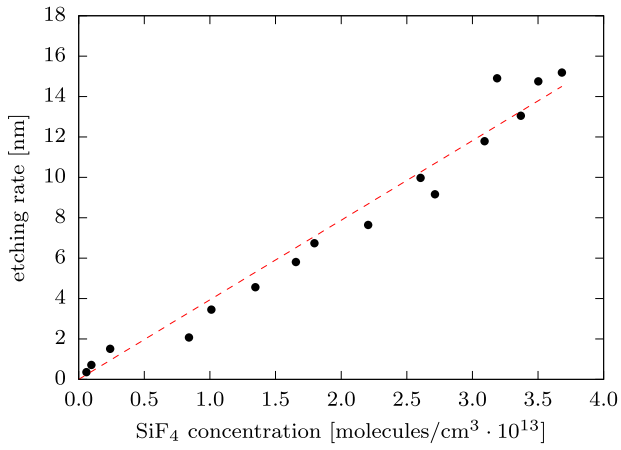

FIG. 5. *Ex situ* determined etching rate depending on the *in situ* measured concentration of SiF_4 averaged over the entire process.

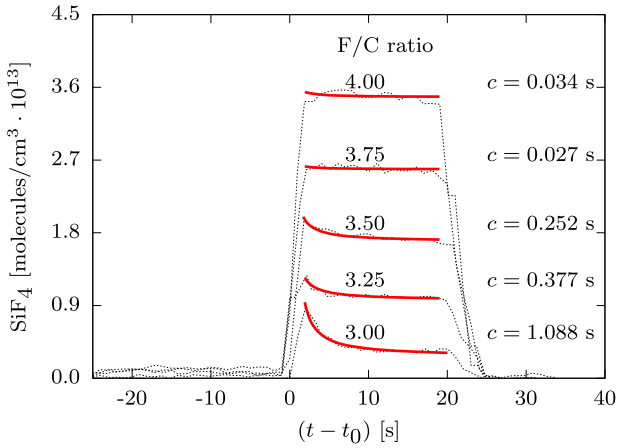

FIG. 6. Time-resolved SiF_4 density measurements at different F/C ratios. A substitution of CF_4 by CHF_3 leads to a significant decay of the SiF_4 density. In addition, the characterization of the time behavior using an exponential decay model (solid lines) is shown together with the corresponding time constant c.

For each Ar flow rate, a decrease of the time constant is observed when the plasma becomes more polymerizing. Therefore, the SiF_4 density decays more slowly to a stationary value at lower F/C ratios. The observation cannot be attributed to the residence time τ of the etching product. According to the relation[3]

$$\tau = \frac{Vp}{\Phi}, \quad (3)$$

with V the chamber volume, p the process pressure, and Φ the precursor flow, τ equals to 0.83 s for a chamber volume of 10.5 l, a process pressure of 100 mTorr, and a flow rate of 100 sccm. The fundamental reason for this behavior is seen in the suppressed desorption of SiF_4 caused by a more dominant adsorption of polymer species on the ULK surface. Thus, the growth of polymer films reduces the production of SiF_4. However, the addition of Ar to the

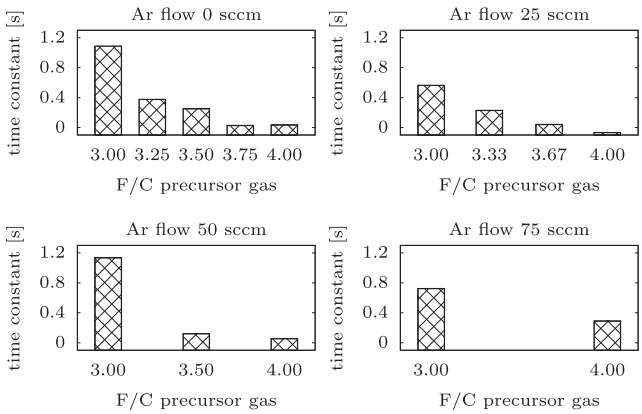

FIG. 7. Exponential time constant c as a function of the F/C ratio for different Ar gas flows. A reduction in the F/C ratio (increase of polymerizing gas) results in higher values for c, i.e., the stationary concentration of the SiF_4 is reached slower at lower F/C ratios.

plasma does not seem to have a straight forward impact on the time constant. For example, for a F/C ratio of 3 and for Ar flows of 0 sccm and 50 sccm, the time constant hardly differs, and it halves roughly for an Ar flow rate of 25 sccm. This effect is currently not well understood and will be the subject of future detailed investigations.

B. Damage depth and polymer thickness

The results extracted out of ellipsometric measurements should follow a certain logic. Actually, this was found in our investigation. Figure 8 shows the results of polymer thickness, damage depth, and the corresponding refractive indices as a function of the F/C ratio for different argon flow rates. First, the found polymer thickness (thickness range: 2 nm up to 13 nm) decreases by increasing the F/C ratio of the precursor gas for each Ar flow. The usage of a higher amount of polymerizing gases leads to thicker polymer films on top of the ULK. Second, the determined refractive indices of the CF films are in a range of 1.21 and 1.96. According to different authors, the refractive index of CF polymer films can take values from 1.15 up to 1.68.[30,31] If the film becomes very similar to polytetrafluoroethylene (PTFE), the refractive index should be in a range of 1.38 and 1.42.[32–34] The high refractive indices are probably caused by the incorporation of aluminum (discussed later in this report; Al source: adapter wafer used during the etch process) into the polymer layer, which is only assumed here. In the case of the ULK damage depth, values between 9 nm and 36 nm were found. The interesting fact is that by increasing the F/C ratio, the damage depth decreases. This seems to be in contrast to the results of other studies, which describe for example PTFE-like layers as protective layers to reduce the ULK damage.[6] However, this only applies in the case of patterning the ULK because the formation of such layers on trench sidewalls could prevent the diffusion of damaging species (e.g., fluorine) in the porous material,[9] while other mechanisms such as EUV/UV irradiation or ion bombardment are less important regarding the patterned ULK damage. In the case of blanket films, the coverage by the polymer film does not suppress the ULK damage. Considering the refractive index of the layer, which represents the damaged regions of partially etched ULK (compare Fig. 2 right), it should be noted that this value shows also a decrease by increasing the F/C ratio. This common decrease implies equally the correctness of the three layer model, which was used to describe the plasma treaded ULK films. Because of the direct proportionality between the dielectric constant and the refractive index, higher damage usually leads to higher refractive indices of the ULK.[8,35]

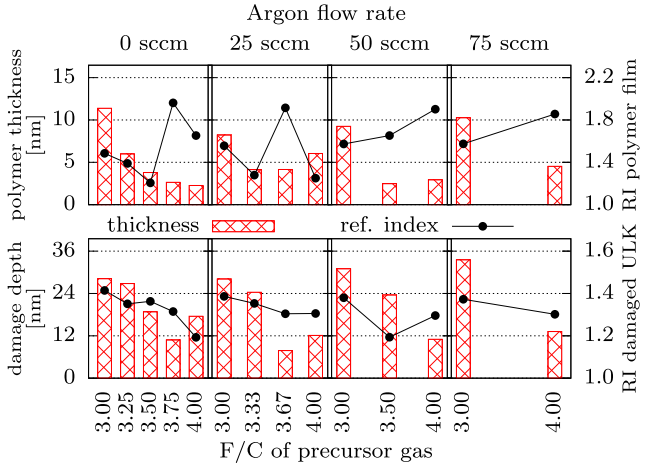

FIG. 8. Effect of different process gas mixtures on the polymer thickness (top diagram, bars), the damage depth (bottom diagram, bars), and the refractive index (RI) (points, right axes), respectively. The polymer thickness as well as the damage depth decreases with the increasing F/C ratio. The drop in the damage depth correlates very well with the refractive index of the layer, which represents the damaged regions in the three layer model.

C. Surface composition of partially etched films

The compositions of the top layers after etching partially at different F/C ratios are shown in Fig. 9. Via XPS, the elements carbon, oxygen, fluorine, silicon, and aluminum on top of the ULK film could be detected. As already mentioned, the source of aluminum is caused by the usage of aluminum coated adapter wafers, which are also exposed to sputtering. Therefore, for the analysis, the aluminum is not considered further. Silicon and oxygen are components of the ULK material. Fluorine should be part of a polymer film. In the case of carbon, it is not immediately obvious, since the polymer films and the ULK material are containing carbon. However, if the trend of the elements for different F/C ratios is considered and compared to each other, it can be noticed that both oxygen and silicon shows an increase. In contrast to this, carbon as well as fluorine drops with increasing F/C ratio. This fact is illustrated with arrows in the diagram of Fig. 9. A scatterplot of carbon surface content vs oxygen surface content over all samples (see Fig. 10, left) shows a strong correlation between them. A high amount of carbon is connected with a small amount of oxygen on top of the partially etched ULK surfaces. This implies that the thicker the polymer film on the ULK, the smaller the signal intensity of ULK components. This fits to the well correlating values of polymer thickness determined by ellipsometry and the carbon content, too. Samples containing a higher carbon amount also exhibited a high polymer thickness, as shown in the right diagram of Fig. 10. These two facts are evidence for the existence of a polymer layer on top of the ULK. By the investigation of the XPS spectra regarding the bonds on top of the ULK film, the polymer fragments C—F, C—F_2, C—F_3, and C—CF_x (x = 1; 2; 3) could be proven. The same bonds were found by Posseme *et al.* after partial etching of ULK in CF_4/Ar/CH_2F_2 plasmas.[17] In contrast to their results, we also found the bond C=O and C—C (or C—H). The latter could be explained by the unavoidable short exposure of the samples to ambient air during the analysis, see also Sec. II D. The bond C=O can be assigned to the polymer film only, since measurements of untreated ULK surfaces do not show this bond. Even on a sample that was sputtered in pure Ar plasma, only a negligible amount of 0.3% was found for this bond.[15] In Fig. 11, each single bond is shown as a function of the F/C ratio of the precursor gas, again for Ar flows of 0 sccm, 25 sccm, 50 sccm, and 75 sccm, respectively. For each Ar flow rate, the C—CF_x bond is the most prominent molecule at the ULK surface after the etching process. In addition, the bonds C—F and C—F_2 show significant percentages of the top layer, while C—F_3 is negligible. Considering only the processes without Ar, it is clearly visible that the species C—F and C—F_2 increase, while C—CF_x decrease by the exchange of CF_4

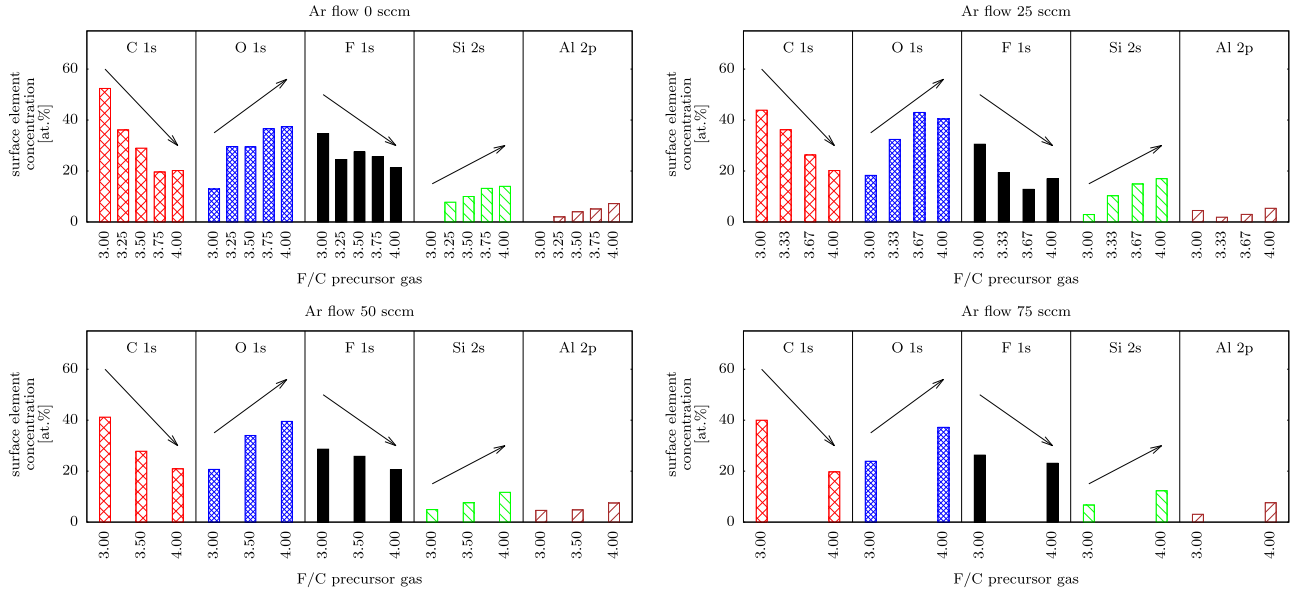

FIG. 9. Surface composition of partially etched ULK films for different F/C ratios and Ar flow rates. The arrows in the diagram illustrate the common drop of carbon and fluorine surface concentrations (attributed to the polymer film) as well as the common increase in silicon and oxygen surface concentrations (attributed to the damaged ULK), which implies a more dominant polymer deposition at lower F/C ratios on the ULK surface. Aluminum is detected because of the usage of aluminum coated adapter wafers.

with CHF_3 (reduction of F/C). Whenever Ar is a part of the process gas, the formation of the bonds seems to be randomly distributed. In addition, the C—F_2 surface concentration becomes smaller, while C—F shows more or less similar surface concentrations. A reason for this can be attributed to the nature of the RIE processes, in particular, to the ion bombardment occurring in such processes. By adding Argon to the process gas, the physical bombardment is enhanced. This may lead to a reduction in the fluorine rich bonds and the film becomes a layer with higher C—CF_x content (relative to C—F_2).[36] Accordingly, no correlation between the precursor gas and the bonds on the surface could be demonstrated. A weak correlation between the precursor gas and the surface bonds was also reported in the study of Li *et al.*[37] The authors evaluated different hydrofluorocarbon precursors with respect to the deposition and etching behavior. Although, they found a high correlation between the CF_2 fraction in the precursor structure and the optical emission signal of CF_2, the correlation between C—F_2 surface density and optical emission of CF_2 was reported as weak. It was justified that the deposition of C—F_2 is less or surface processes modify chemical moieties. The ion bombardment can also lead to etching and activation of the polymeric surface. Both mechanisms could reduce the fluorine content of the polymer film, too.[38] The fluorine content reduction induced by ion bombardment could explain the significant rise in the C—C bond in the presence of Ar. Additionally, it is known that the Ar dilution of the process gas leads to the formation of polymer films with a lower fluorine content.[8] The fact that the bond energy of C—C/C—H could also correspond to ULK, may lead to the assumption, that a thinner polymer film on top of the ULK causes the increase of this signal. Nevertheless, the sample from top to down consists out of the polymer film and damaged ULK underneath. However, the damaged ULK should not include C—H bonds. First, Posseme *et al.* discussed that, indeed, ion bombardment can break the C—H bonds of ULK surfaces.[17] In addition, Rakhimova *et al.* attributed the presence of the C—H bonds to some contaminations of the ULK surface and reported the disappearance of C—H, if the surface is exposed to fluorine atoms.[11] Both occur in a RIE process, so that the C—C/C—H peak can be assigned to the polymer film on top of the ULK. This result of film characteristics demonstrates the existence of a polymer film on top of the ULK after the etch process. Thus, again it is confirmed to use a 3 layer model for the VASE measurements.

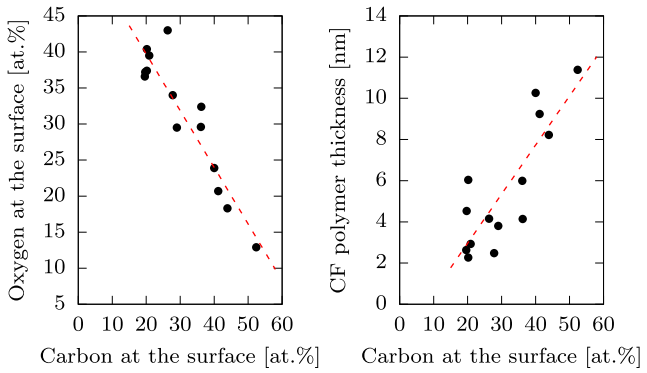

FIG. 10. The correlation of oxygen and carbon indicates a thicker polymer film if less amount of oxygen is detected on the surface (left diagram). The scatter plot of polymer thickness (VASE-measurement) vs carbon content at the partially etched ULK surface provides an evidence.

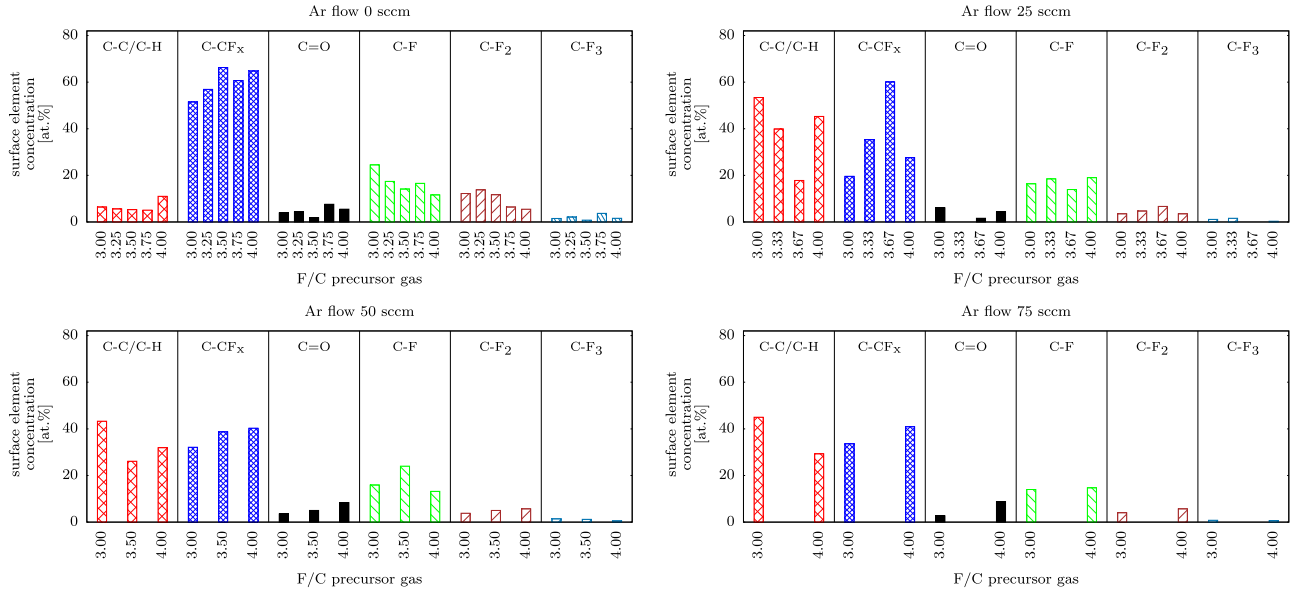

FIG. 11. Bonds on partially etched ULK surfaces for different F/C ratios and Ar flow rates. Typical bonds such as C—CF_x, CF, CF_2, and CF_3 were found after the plasma treatment. More details are given in the text.

D. Correlation analysis of process results

Further investigations regarding the correlation of different film components and process results are done by calculating the Pearson correlation coefficient between each other. In the case of the existence of a dependency of two variables, the coefficient delivers values close to 1 and −1, respectively. While a value of 1 describes a common rise of both variables, −1 indicates the opposite behavior of the considered parameters. For example, the data of the scatter plots in Fig. 10 result in the correlation coefficients of −0.921 (left) and 0.717 (right), respectively.

Figure 12 shows the result of the correlation analysis. The diagram shows the calculated Pearson correlation coefficients of the film composition to the determined process results. The plot can be separated into two parts, the film components on the left and the chemical bonds on the right side. It is seen that the correlation between the chemical bonds and the process results etch rate, polymer thickness, damage depth, and time constant is very weak. Therefore, it cannot be assumed that a dependency between the molecular structure of the polymer film and the process results exists. In contrast to this, the film components exhibit strong correlations to the process results. It should be emphasized here that

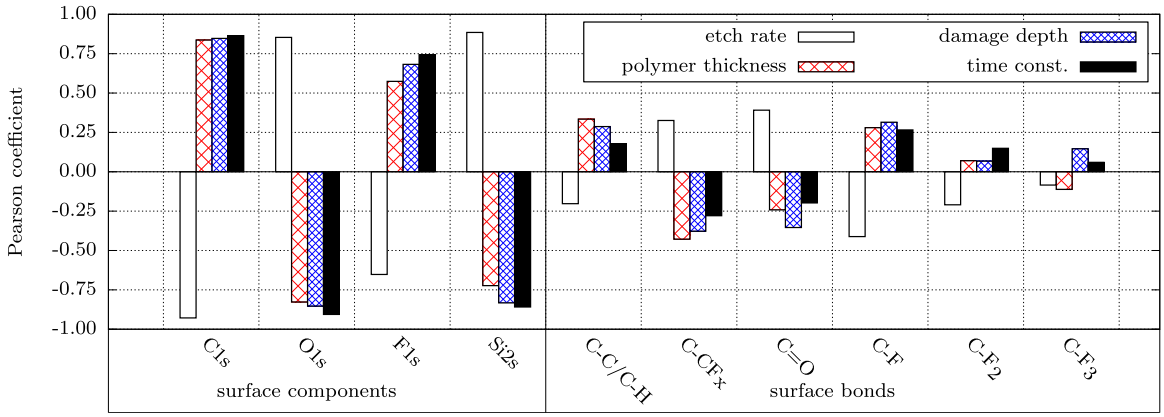

FIG. 12. Correlation analyses of the process results with XPS data. Significant correlations are present for the atomic components, while only weak correlations were found for the molecular bonds. The comparable coefficients for the time constant and for the ellipsometric results (polymer thickness and damage depth) suggest a mutual dependence.

especially the etch rate shows a very high correlation to the atomic film composition. While the coefficient for oxygen and silicon is positive, negative values were found for carbon and fluorine. As discussed above, the etching is suppressed caused by polymerization on top of the ULK surface. Furthermore, the same can be seen considering the correlation between the components and the polymer thickness measured by ellipsometry. More astonishing is the fact that the polymer thickness, damage depth, and the time constant extracted from the temporal behavior of the *in situ* measurements of SiF_4 show for each component a similar correlation coefficient. This suggests a mutual dependence between each of these properties.

The following two diagrams in Fig. 13 show the *in situ* determined time constant as a function of the *ex situ* measured polymer thickness and damage depth, respectively. In the upper plot, the common rise of the polymer thickness and c is clearly visible. To guide the eyes, a linear function has been fitted to the data and plotted using a solid line. The fundamental reason for the temporal behavior of the SiF_4 density is interpreted as the increasing suppressed desorption of SiF_4 caused by a more dominant adsorption of polymer species on the ULK surface. Therefore, the growth of polymer films reduces the formation of the etching product SiF_4 over time. In addition, for the depth of the damaged zone, a monotonic increase with increasing values for the decay time up to about 0.7 s was found (bottom diagram of Fig. 13). For larger time constants, this effect seems to saturate to a damage depth in the range of 30 nm. A second order polynomial has been fitted to the data to guide the eyes (solid line). It should be noticed that we do not discuss here a functional dependency between these two properties. However, the correlation of ULK damage and an *in situ* measure is a quite interesting fact. In addition, Zimmermann *et al.* reported a correlation between ULK damage and *in situ* QCLAS measurements.[6] They found a link between the ULK sidewall damage and the measured stationary CF_2 density during the patterning process.

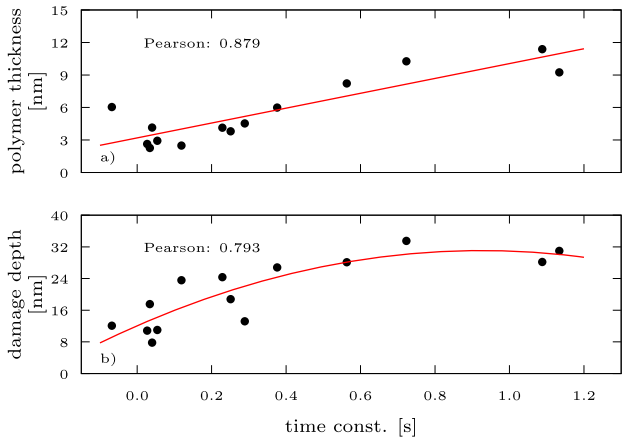

FIG. 13. The temporal behavior of the SiF_4 concentration characterized by its exponential time constant c correlates with the polymer thickness (a) and with the damage depth of partial etched ULK (b). In both graphs, a fit to the data is plotted to guide the eyes (solid line) – graph (a): linear function; graph (b): second order polynomial.

However, the author did not discuss a causality and just mentioned the weak correlation between these parameters. From the observed behavior shown in Fig. 13, one may see different influences of damaging processes caused by radicals, ions, and VUV/UV radiation, respectively. As pointed out by Uchida *et al.*, the ions play a dominant role in increasing the dielectric constant of porous SiOCH, i.e., an increase in the damage.[14] The influence of radicals should decrease with increasing CF film thickness on top of the SiOCH layer even if the film has comparable porosity. Furthermore, as reported by Uchida *et al.*, VUV radiation was found to penetrate to a depth of about 23 nm in a porous SiOCH film, which is close to the saturated values of the damage depth observed for time constants larger than 0.7 s. The increasing values for increasing time constants below 0.7 s may be attributed to a change in the photon flux in the VUV and UV with decreasing F/C ratio. It has been shown by Rakhimova *et al.* that the formation of CF_2, the most prominent radical in fluorocarbon plasmas, is enhanced with decreasing F/C ratio, resulting in a larger UV photon flux by a factor of 4.[39] All these processes may clearly be hampered and limited due to the thickness of a CF polymer film on top of the damaged SiOCH layer. However, these results demonstrate the feasibility to monitor the ULK damage during the etching process of ULK.

IV. CONCLUSION

In this study, ultra low-k dry etching processes were analyzed by quantum cascade laser absorption spectroscopy. The concentration of the etching product SiF_4 was measured during etching processes with varying gas mixtures. According to expectations, a strong correlation between the etching rate and SiF_4 density was found. In addition, a non-linear temporal behavior during the process of the density of this plasma species was observed. This temporal behavior could be characterized using an empirical model for an exponential decay. A physical interpretation of the model is a subject of further investigations. While the SiF_4 density reaches its maximum value with plasma ignition, it decays to a stationary value over the process time. The stationary concentration is achieved sooner by increasing the F/C ratio of the precursor gas. Detailed analyses were performed to clarify the temporal behavior of the SiF_4 density, whereby Variable Angle Ellipsometry and X-ray Photoelectron Spectroscopy were used to analyze the partially etched ULK surfaces. A three layer model was developed to describe the ellipsometric data, in order to take into account polymer deposition and ULK damage, which occur during the etching process. The model provided the thickness of the polymer layer on top of the ULK, and it was depicted that a reduction in the F/C ratio of the precursor gas leads to thicker polymer films. A similar correlation was found for the damage depth too. Higher damage has been established by decreasing the F/C ratio. The existence of polymer layers on top of partially etched ULK films could be proven by XPS. The found correlation between carbon and oxygen surface concentrations shows that surfaces with high carbon content contain less oxygen, which is well in line with the determined polymer thicknesses. In addition, typical components of polymer films (C—F, C—F_2, C—F_3) could be detected.

In contrast to the element surface concentrations of the partially etched surfaces, the surface bonds only correlate with the F/C

ratio of the precursor gas, if no argon is present in the plasma. The weak correlation of chemical surface bonds with the F/C ratio, the damage depth, polymer thickness, and SiF_4 time constant is attributed to the ion bombardment during the etching process. Via correlation analysis, it was successfully extracted that the temporal behavior of the SiF_4 density is caused by a polymer deposition taking place during the etching process using fluorocarbon gases. Therefore, the time dependency of the SiF_4 density observed in this study can be explained. The decay of the SiF_4 density during the duration of the process is caused by the suppressed desorption of SiF_4 molecules due to a more dominant adsorption of polymers on the ULK surface. Thus, the growth of polymer films hampers the formation of the etching product SiF_4. The sooner the stationary SiF_4 density is achieved, the thinner the polymer film on top of the ULK. This can be predicted quantitatively by the decay time constant of the SiF_4 density. It was also observed that the ULK damage is saturated with respect to the depth of the damaged zone for sufficiently small F/C ratios, which corresponds to large time constants for the decay of the SiF_4 density.

Finally, the study demonstrates the feasibility of deriving sample properties directly from *in situ* density measurements of molecular plasma species. The plasma chemistry and the concentration of suitable species contain essential information about the process and its result. This demonstrates the possibility of being able to measure parameters of processed samples *in situ* in the future, which would otherwise be difficult to access in production.

ACKNOWLEDGMENTS

The authors acknowledge H. Zimmermann and U. Macherius for their continuous support. This work was partly funded by the European Union and the German Federal Ministry of Education and Research in the ECSEL project SeNaTe (Grant Agreement No. 662338, Promotional Reference No. 16ESE0044S).

DATA AVAILABILITY

The data that support the findings of this study are openly available in INPTDAT at https://doi.org/10.34711/inptdat.194.

REFERENCES

[1]M. Klick, M. Kammeyer, W. Rehak, W. Kasper, P. Awakowicz, and G. Franz, "Innovative plasma diagnostics and control of process in reactive low-temperature plasmas," Surf. Coat. Technol. **98**, 1395–1399 (1998).

[2]K. H. Baek, Y. Jung, G. J. Min, C. Kang, H. K. Cho, and J. T. Moon, "Chamber maintenance and fault detection technique for a gate etch process via self-excited electron resonance spectroscopy," J. Vac. Sci. Technol., B **23**, 125 (2005).

[3]G. Franz, *Low Pressure Plasmas and Microstructuring Technology*, 1st ed. (Springer Publishing Company, Incorporated, 2009).

[4]K. H. Baek, E. Lee, M. Klick, and R. Rothe, "Comprehensive understanding of chamber conditioning effects on plasma characteristics in an advanced capacitively coupled plasma etcher," J. Vac. Sci. Technol., A **35**, 021304 (2017).

[5]N. Lang, S. Zimmermann, H. Zimmermann, U. Macherius, B. Uhlig, M. Schaller, S. E. Schulz, and J. Röpcke, "On treatment of ultra-low-k SiCOH in CF_4 plasmas: Correlation between the concentration of etching products and etching rate," Appl. Phys. B **119**, 219–226 (2015).

[6]S. Zimmermann, M. Haase, N. Lang, J. Röpcke, S. E. Schulz, and T. Otto, "The role of plasma analytics in leading-edge semiconductor technologies," Contrib. Plasma Phys. **58**, 367–376 (2018).

[7]M. Hübner, N. Lang, S. Zimmermann, S. E. Schulz, W. Buchholtz, J. Röpcke, and J. H. van Helden, "Quantum cascade laser based monitoring of CF_2 radical concentration as a diagnostic tool of dielectric etching plasma processes," Appl. Phys. Lett. **106**, 1–5 (2015).

[8]M. R. Baklanov, J.-F. de Marneffe, D. Shamiryan, A. M. Urbanowicz, H. Shi, T. V. Rakhimova, H. Huang, and P. S. Ho, "Plasma processing of low-k dielectrics," J. Appl. Phys. **113**, 041101 (2013).

[9]M. Baklanov, A. Urbanowicz, G. Mannaert, and S. Vanhaelemeersch, "Low dielectric constant materials: Challenges of plasma damage," in *2006 8th International Conference on Solid-State and Integrated Circuit Technology Proceedings* (IEEE, 2006), pp. 291–294.

[10]J. Bao, H. Shi, J. Liu, H. Huang, P. S. Ho, M. D. Goodner, M. Moinpour, and G. M. Kloster, "Mechanistic study of plasma damage of low k dielectric surfaces," J. Vac. Sci. Technol., B **26**, 219 (2008).

[11]T. V. Rakhimova, D. V. Lopaev, Y. A. Mankelevich, A. T. Rakhimov, S. M. Zyryanov, K. A. Kurchikov, N. N. Novikova, and M. R. Baklanov, "Interaction of F atoms with SiOCH ultra-low-k films: I. Fluorination and damage," J. Phys. D: Appl. Phys. **48**, 175203 (2015).

[12]T. Oszinda, M. Schaller, D. Fischer, C. Walsh, and S. E. Schulz, "Investigation of physical and chemical property changes of ultra low-κ SiOCH in aspect of cleaning and chemical repair processes," Microelectron. Eng. **87**, 457–461 (2010).

[13]T. Fischer, N. Ahner, S. Zimmermann, M. Schaller, and S. E. Schulz, "Influence of thermal cycles on the silylation process for recovering k-value and chemical structure of plasma damaged ultra-low-k materials," Microelectron. Eng. **92**, 53–58 (2012).

[14]S. Uchida, S. Takashima, M. Hori, M. Fukasawa, K. Ohshima, K. Nagahata, and T. Tatsumi, "Plasma damage mechanisms for low-k porous SiOCH films due to radiation, radicals, and ions in the plasma etching process," J. Appl. Phys. **103**, 073303 (2008).

[15]T. V. Rakhimova, D. V. Lopaev, Y. A. Mankelevich, K. A. Kurchikov, S. M. Zyryanov, A. P. Palov, O. V. Proshina, K. I. Maslakov, and M. R. Baklanov, "Interaction of F atoms with SiOCH ultra low-k films. Part II: Etching," J. Phys. D: Appl. Phys. **48**, 175204 (2015).

[16]S. Lee, J. Woo, D. Jung, J. Yang, J.-h. Boo, H. Kim, and H. Chae, "Effect of etching on dielectric constant and surface composition of SiCOH low-k films in inductively coupled fluorocarbon plasmas," Thin Solid Films **517**, 3942–3946 (2009).

[17]N. Posseme, T. Chevolleau, O. Joubert, L. Vallier, and N. Rochat, "Etching of porous SiOCH materials in fluorocarbon-based plasmas," J. Vac. Sci. Technol., B **22**, 2772 (2004).

[18]H. Fujiwara, *Spectroscopic Ellipsometry: Principles and Applications* (Wiley, 2007), p. 388.

[19]S. Eslava, G. Eymery, P. Marsik, F. Iacopi, C. E. A. Kirschhock, K. Maex, J. A. Martens, and M. R. Baklanov, "Optical property changes in low-k films upon ultraviolet-assisted curing," J. Electrochem. Soc. **155**, G115 (2008).

[20]P. Marsik and M. R. Baklanov, "Optical characteristics and UV modification of low-k materials," in *2008 9th International Conference on Solid-State and Integrated-Circuit Technology* (IEEE, 2008), pp. 765–768.

[21]P. Marsik, P. Verdonck, D. De Roest, and M. R. Baklanov, "Porogen residues detection in optical properties of low-k dielectrics cured by ultraviolet radiation," Thin Solid Films **518**, 4266–4272 (2010).

[22]K. Nishida, K. Ono, and K. Eriguchi, "Optical model for spectroscopic ellipsometry analysis of plasma-induced damage to SiOC films," Jpn. J. Appl. Phys. **56**, 06HD01 (2017).

[23]N. Vandencasteele and F. Reniers, "Plasma-modified polymer surfaces: Characterization using XPS," J. Electron Spectrosc. Relat. Phenom. **178-179**, 394–408 (2010).

[24]M. Haase, R. Ecke, and S. E. Schulz, "Requirements and challenges on an alternative indirect integration regime of low-k materials," in *AMC 2015 Advanced Metallization Conference* (Chemnitz University of Technology, 2016), https://nbn-resolving.org/urn:nbn:de:bsz:ch1-qucosa-207219.

[25]R. Leitsmann, O. Böhm, P. Plänitz, C. Radehaus, M. Schaller, and M. Schreiber, "Dissolution of CF-polymer films at ultra low-k surfaces using diluted HF," ECS J. Solid State Sci. Technol. **1**, N14–N17 (2012).

[26]J. F. Moulder, W. F. Stickle, P. E. Sobol, and K. D. Bomben, *Handbook of X-Ray Photoelectron Spectroscopy: A Reference Book of Standard Spectra for Identification and Interpretation of XPS Data* (Physical Electronics Division, Perkin-Elmer Corporation, 1995).
[27]M. A. Sobolewski and C. R. Helms, "X-ray photoelectron spectroscopy and auger spectroscopy studies of thin silicon nitride films thermally grown on silicon," J. Vac. Sci. Technol., A **6**, 1358–1362 (1988).
[28]C. D. Wagner, L. E. Davis, and W. M. Riggs, "The energy dependence of the electron mean free path," Surf. Interface Anal. **2**, 53–55 (1980).
[29]J. C. Ashley and C. J. Tung, "Electron inelastic mean free paths in several solids for 200 eV ≤ E ≤ 10 keV," Surf. Interface Anal. **4**, 52–55 (1982).
[30]H. Jiang, K. O'Neill, J. T. Grant, S. Tullis, K. Eyink, W. E. Johnson, P. Fleitz, and T. J. Bunning, "Variable refractive index polymer thin films prepared by plasma copolymerization," Chem. Mater. **16**, 1292–1297 (2004).
[31]T. C. Nason, J. A. Moore, and T. M. Lu, "Deposition of amorphous fluoropolymer thin films by thermolysis of Teflon amorphous fluoropolymer," Appl. Phys. Lett. **60**, 1866–1868 (1992).
[32]J. Elders, H. V. Jansert, and M. Elwenspoek, "Materials analysis of fluorocarbon films for MEMS applications," in *Proceedings, IEEE Micro Electro Mechanical Systems: An Investigation of Micro Structures, Sensors, Actuators, Machines and Robotic Systems* (IEEE, 1994), pp. 170–175.
[33]S. Vaswani, J. Koskinen, and D. W. Hess, "Surface modification of paper and cellulose by plasma-assisted deposition of fluorocarbon films," Surf. Coat. Technol. **195**, 121–129 (2005).
[34]S. Agraharam, D. W. Hess, P. A. Kohl, and S. A. Bidstrup Allen, "Electrical properties and temperature-humidity studies of fluorocarbon films deposited from pentafluoroethane/argon plasmas," J. Electrochem. Soc. **148**, F102 (2001).
[35]S. Zimmermann, N. Ahner, F. Blaschta, M. Schaller, H. Rülke, S. E. Schulz, and T. Gessner, "Analysis of the impact of different additives during etch processes of dense and porous low-k with OES and QMS," Microelectron. Eng. **87**, 337–342 (2010).
[36]G. S. Oehrlein, Y. Zhang, D. Vender, and M. Haverlag, "Fluorocarbon highdensity plasmas. I. Fluorocarbon film deposition and etching using CF_4 and CHF_3," J. Vac. Sci. Technol., A **12**, 323–332 (1994).
[37]C. Li, R. Gupta, V. Pallem, and G. S. Oehrlein, "Impact of hydrofluorocarbon molecular structure parameters on plasma etching of ultra-low-k dielectric," J. Vac. Sci. Technol., A **34**, 031306 (2016).
[38]S. J. Limb, C. B. Labelle, K. K. Gleason, D. J. Edell, and E. F. Gleason, "Growth of fluorocarbon polymer thin films with high CF_2 fractions and low dangling bond concentrations by thermal chemical vapor deposition," Appl. Phys. Lett. **68**, 2810 (1995).
[39]T. V. Rakhimova, O. V. Braginsky, K. S. Klopovskiy, A. S. Kovalev, D. V. Lopaev, O. V. Proshina, A. T. Rakhimov, D. Shamiryan, A. N. Vasilieva, and D. G. Voloshin, "Experimental and theoretical studies of radical production in RF CCP discharge at 81-MHz frequency in Ar/CF_4 and Ar/CHF_3 mixtures," IEEE Trans. Plasma Sci. **37**, 1683–1696 (2009).